

Effects of electrochemical parameters on electropolymerisation of 2-nitro-p-phenylenediamine synthesised in an acidic medium

Ahmad S. Barham^{1,*}, and Mohammad A. Kanan²

¹ General Subjects Department, College of Engineering (CE), University of Business and Technology (UBT), Jeddah 21448, Kingdom of Saudi Arabia

² Industrial Engineering Department, College of Engineering (CE), University of Business and Technology (UBT), Jeddah 21448, Kingdom of Saudi Arabia

*E-mail: ahmad.s@ubt.edu.sa

Received: 27 January 2020 / Accepted: 22 March 2020 / Published: 10 May 2020

Electrochemical cyclic voltammetry (CV) was used to synthesise poly 2-nitro-p-phenylenediamine (2NPPD) as a thin film, on either 1.6 mm diameter gold electrodes ($A= 0.02 \text{ cm}^2$) or on 3.0 mm glassy carbon ($A= 0.07 \text{ cm}^2$) in 0.1 mol dm^{-3} sulfuric acid (pH 1.2). This study explores the electropolymerisation process of poly 2NPPD-modified electrodes, using a general factorial design. The morphological properties of the formed polymer were subsequently examined using scanning electron microscopy (SEM). Tree-like structures, with faint scratches, were observed on the electrode's surfaces. Interactions between the factors of scan rates and the type of electrode materials were both investigated. The rapid drop in the current, in all CV measurements, was proposed as an indication of electropolymerisation. Anodic current peak densities were selected as the response in the design study and, in order to ensure reproducibility, each run in this study was performed in triplicate. This study proposes the mechanism of the electrochemical polymerisation reaction. The diffusion coefficients were measured using the Randles-Sevcik equation, which confirmed that the electropolymerisation of the 2NPPD monomer is a linear diffusion-controlled process. When the concentration of the 2NPPD monomer was decreased, calculated diffusion coefficients also decreased.

Keywords: electropolymerisation; poly(2-nitro-p-phenylenediamine) (2NPPD); general factorial design; electrochemical cyclic voltammetry (CV); diffusion.

1. INTRODUCTION

A thin film of polymer can be grown on several conducting or semiconducting surfaces, by means of electropolymerisation [1-7]. Essentially, electropolymerisation can be achieved anodically, when the monomer gives an electron to the anode through an oxidation process. This can also be achieved cathodically, when the monomer attracts an electron from the cathode, through a reduction process [8].

The electropolymerisation of aniline derivatives have attracted the attention of several researchers [9-14]. Vanossi et al. explore the physico-chemical characteristics of thin poly-(ortho-phenylenediamine) films, which are obtained by electrochemical oxidation of the relevant monomer by cyclic voltammetry (CV) [7]. Sayyah et al. examine the electropolymerisation and characterisation of a binary mixture of *o*-phenylenediamine and 2-aminobenzothiazole on a Pt electrode from an aqueous HCl solution, using the CV technique [8]. Yu and Khoo similarly investigate the anodic electropolymerisation of 4-nitro-1,2-phenylenediamine (4NoPD) in different supporting electrolytes with different pH, on gold and glassy carbon electrodes. Focusing particularly on the feasibility of electropolymerisation of 4NoPD and the electrochemical behaviours of the polymer film that is formed [9], the authors report that the pH of the electropolymerisation medium, the nature of the background electrolyte, and the number of cycles used all strongly affected the amount of polymer that was deposited [9]. In another study, these same authors also investigated the electropolymerisation and characterisation of a binary mixture of 3-chloro-aniline and 2-amino-phenyl-thiazole on a Pt electrode in an acidic medium, under different reaction conditions. In this study, they obtained a block copolymer film on a Pt electrode [15]. Mousa et al. have fabricated improved sensitivity biosensors of conductive polyaniline nanofibers and poly(aniline-*co*-*N*-phenyl-*o*-phenylenediamine) nano-flakes, through an electropolymerisation potentiodynamic CV technique [16].

2NPPD is a reddish-brown crystalline powder that is used in personal care and cosmetics, such as hair dye formulations. It is a non-oxidative coal-tar dye in semi-permanent hair dye formulations and an oxidative permanent tinting colour. Moreover, although 2NPPD is not an oxidation dye, it is present in oxidation formulations, as a colour tinting agent [17].

Currently, the electrochemical properties of 2-nitro-*p*-phenylenediamine (2NPPD) have not been extensively studied in the literature. Therefore, the current study was conducted to enhance our understanding of the electrochemical behaviour of this compound. The main objective of this present work is to explore the electrochemical properties of 2NPPD by CV in an acidic medium, through a general factorial design. The design was constructed to engage with the electropolymerisation event. Scan rates and the electrode's type of materials were examined, as were their interactions. The first current anodic peak densities were selected as the response obtained by the first CV cycle, and the morphology of the obtained thin film polymers were shown. The diffusion coefficients were calculated using the Randles-Sevcik equation and the electrochemical mechanism of the polymerisation reaction has been proposed.

2. EXPERIMENT

2.1. Materials and Reagents

All chemicals were used as they were received. The 2NPPD, potassium ferrocyanide trihydrate (>98%), potassium chloride (99%), and potassium ferricyanide (>98%) were all purchased from Alfa Aesar, Germany. Sulfuric acid (95–98%) was procured from PRS, Panreac, Spain. All aqueous solutions were prepared using deionised water from a Milli-pore Milli-Q system (resistivity= 18.2 MΩ cm).

2.2. Film Preparation

All electrochemical experiments were conducted using an EZstat-Pro potentiostat manufactured by NuVant Systems Inc. (IN, USA), which was equipped with EZware 2013 V7 analysis software, with a three electrode glass cell.[18]

Prior to the electrochemical experiments, the working electrode (gold or glassy carbon) was mechanically polished for two minutes, using the suspended solution of 0.05 μm alumina. This was performed with polishing pads (polishing kit number: PK-4) that were purchased from BASi Preclinical services (IN, USA). The working electrode was immediately flushed with excess deionised water to remove any remaining alumina deposits. A platinum coiled wire (230 mm), which was mounted in a CTFE[®] cylinder, was used as the counter electrode and Ag/AgCl (3 mol dm⁻³ KCl) was used as a reference electrode. All the electrodes were supplied by BASi (IN, USA). [18]

The cleaned and polished electrodes were tested before the electropolymerisation experiments, by performing CV runs that operated between -0.2 V and 0.6 V (six cycles), in a solution of 20 mmol dm⁻³ K₃Fe(CN)₆/ K₄Fe(CN)₆. This consisted of 0.1 mol dm⁻³ KCl vs. (Ag/AgCl, 3 mol dm⁻³ KCl), at a sweep rate of 20 mV s⁻¹. [18]

The 2NPPD monomer was electropolymerized at polished 1.6 mm diameter gold electrodes ($A=0.02\text{ cm}^2$) or 3 mm glassy carbon ($A=0.07\text{ cm}^2$). The concentration of the 2NPPD monomer of 5 or 10 mmol dm⁻³ was prepared in 0.1 mol dm⁻³ sulfuric acid solution, as a supporting electrolyte.

The solutions were then electropolymerized vs. (Ag/AgCl, 3.0 mol dm⁻³ KCl), by applying the sweeping potential between 0.0–1.0 V. The electrochemical polymerisation was performed by CV, using 20 cycles of the mentioned potential region. Several scan rates, ranging from 5 to 30 mV s⁻¹, were used in the experiments.

At the end of each electropolymerisation experiment, all the modified electrodes were tested in a solution of 20 mmol dm⁻³ K₃Fe(CN)₆/ K₄Fe(CN)₆, which consisted of 0.1 mol dm⁻³ KCl vs. (Ag/AgCl, 3 mol dm⁻³ KCl), at a sweep rate of 20 mV s⁻¹ for six sweeps of the applied potential. This step was performed to ensure that the polymer film was deposited at the electrode surface.

A gold-coated silicon wafer (Au.1000.SL1), with a layer of 100 nm gold and 5 nm titanium thicknesses, was purchased from Platypus Technologies (Madison, USA). The gold-coated Si wafer was cut into small chips of 1.0 cm \times 1.0 cm, using the LatticeAx[™] 120 from LatticeGear (USA). These were then used as working electrodes in the electropolymerisation of 2NPPD, as described in the previous section. The morphology of the modified gold-coated Si-chip ($A=1.0\text{ cm}^2$) surfaces was inspected using an ULTRA 55 ZEISS scanning electron microscope (Germany). The samples were mounted on a metallic stub with a double-sided adhesive tape, prior to the scanning electron microscopy (SEM) capturing process. The electronic images were captured at an applied acceleration potential of 5 kV, using a highly efficient In-lens SE detector and at a working distance of 4.0 mm.

2.3. Construction of the Design of the Experiments (DOE)

A general factorial design of the experiment was carried out to investigate the interactions between the operating parameters on the electropolymerisation of 2NPPD, which was prepared in an

acidic medium. Using CV, the scan rate and type of the electrode's materials were selected to examine their effects on the electropolymerisation process. The selected response was the first anodic peak current densities that were obtained from the first CV cycle in each run. In order to ensure reproducibility, each run in this study was performed in triplicate. These responses were analysed using Design Expert 7.0.0. (Stat-Ease, Inc., USA). Table 1 presents the general factorial matrix that was conducted in this study, along with the output values of each run. The first factor was the scan rate, and six levels of scan rates were used: namely, 5, 10, 15, 20, 25, and 30 mV/s. The second factor was the electrode's materials, and two levels of electrode's materials were selected: namely, gold and glassy carbon. Tables II and III present the levels of study that are the focus of this study.

Table 1. Experimental data along with standard order and run as per DOE matrix.

Standard order	Run	Factor 1: Scan Rate (mV)	Factor 2: Electrode's Type	Response: First anodic peak current density ($\mu\text{A}/\text{cm}^2$)
5	1	10	Gold	614
33	2	25	Glassy C	1501
12	3	20	Gold	990
18	4	30	Gold	1453
19	5	5	Glassy C	501
11	6	20	Gold	1091
16	7	30	Gold	1434
29	8	20	Glassy C	1210
20	9	5	Glassy C	463
2	10	5	Gold	324
7	11	15	Gold	847
36	12	30	Glassy C	1671
28	13	20	Glassy C	1261
10	14	20	Gold	1025
27	15	15	Glassy C	1108
24	16	10	Glassy C	811
6	17	10	Gold	580
4	18	10	Gold	832
21	19	5	Glassy C	491
31	20	25	Glassy C	1316
9	21	15	Gold	869
23	22	10	Glassy C	806
13	23	25	Gold	1135
8	24	15	Gold	883
14	25	25	Gold	1161
30	26	20	Glassy C	1309
34	27	30	Glassy C	1591
22	28	10	Glassy C	848
25	29	15	Glassy C	1084

32	30	25	Glassy C	1529
17	31	30	Gold	1429
3	32	5	Gold	394
15	33	25	Gold	1219
1	34	5	Gold	506
35	35	30	Glassy C	1696
26	36	15	Glassy C	1092

Table 2. Factors of scan rate and factor levels (Number of levels: 6)

Scan Rate (mV)	A[1]	A[2]	A[3]	A[4]	A[5]
5	1	0	0	0	0
10	0	1	0	0	0
15	0	0	1	0	0
20	0	0	0	1	0
25	0	0	0	0	1
30	-1	-1	-1	-1	-1

Table 3. Factors of electrode's type materials and factor levels (Number of levels: 2)

Electrode's Type	B[1]
Gold (G)	-1
Glassy Carbon (GC)	1

3. RESULTS AND DISCUSSION

Figure 1 presents the CV curves that are linked to the electropolymerisation of 5 mmol dm^{-3} 2NPPD, using gold electrodes (Figure 1A) and glassy carbon electrodes (Figure 1B), both of which were prepared in 0.1 mol dm^{-3} sulfuric acid ($\text{pH}=1.2$). The electrode's areas for the gold and glassy carbon electrodes were $A= 0.02 \text{ cm}^2$, $A= 0.07 \text{ cm}^2$, respectively. All potentials were measured versus Ag/AgCl (3 mol dm^{-3} KCl) for several scan rates, ranging from 5 to 30 mV/s, for 25 sweeps. The first and second sweeps are presented in Figure 1, for every scan rate that was used.

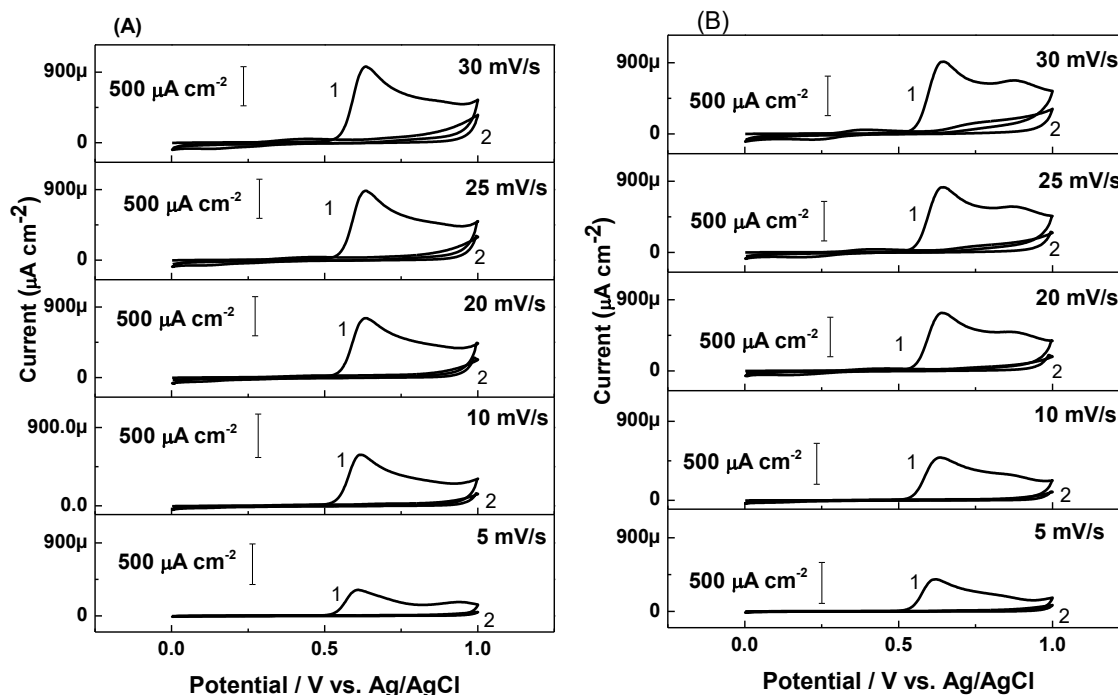


Figure 1. Electropolymerisation in $0.1 \text{ mol dm}^{-3} \text{ H}_2\text{SO}_4$ at $\text{pH}=1.2$ of 5 mmol dm^{-3} 2-nitro-phenylenediamine (2NPPD) vs Ag/AgCl (3 mol dm^{-3} KCl). Cyclic voltammograms were obtained at a scan rate of 5 up to 30 mV s^{-1} (25 cycles) using (A) a bare 1.6 mm gold electrode ($A=0.02 \text{ cm}^2$) and (B) a bare 3 mm glassy carbon electrode ($A=0.07 \text{ cm}^2$). This figure presents the first and second cycles for every scan rate.

In the first cycle of each scan rate, an anodic oxidation peak was observed at a range of 0.55 to 0.65 V. Current density values of $450 \text{ } \mu\text{A}/\text{cm}^2$ were obtained for the 5mV scan rate, and $900 \text{ } \mu\text{A}/\text{cm}^2$ was obtained at the 30mV scan rate. As Figure 1 illustrates, an irreversible oxidation reaction had occurred at the electrode's surface, which was noted from the disappearance of the first anodic peak in the subsequent cycles.

Figure 2 presents CV curves that are associated to the electropolymerisation of 10 mmol dm^{-3} 2NPPD, using gold electrodes (Figure 2A) and glassy carbon electrodes (Figure 2B), which were both prepared in 0.1 mol dm^{-3} sulfuric acid ($\text{pH}=1.2$). The same CV experimental parameters were used to construct Figure 2 as were used to construct Figure 1. CVs were conducted up to 25 sweeps, and the first and second sweeps are presented in Figure 2 for every scan rate that was used.

In the first cycle of each scan rate, an anodic oxidation peak was observed, at a range of 0.55 to 0.65 V. Current density values of $550 \text{ } \mu\text{A}/\text{cm}^2$ were obtained for the 5mV scan rate and $1500 \text{ } \mu\text{A}/\text{cm}^2$ was obtained at the 30mV scan rate. An irreversible oxidation reaction had occurred at the electrode's surface, which was noted from the disappearance of the first anodic peak in the subsequent cycles (Figure 2).

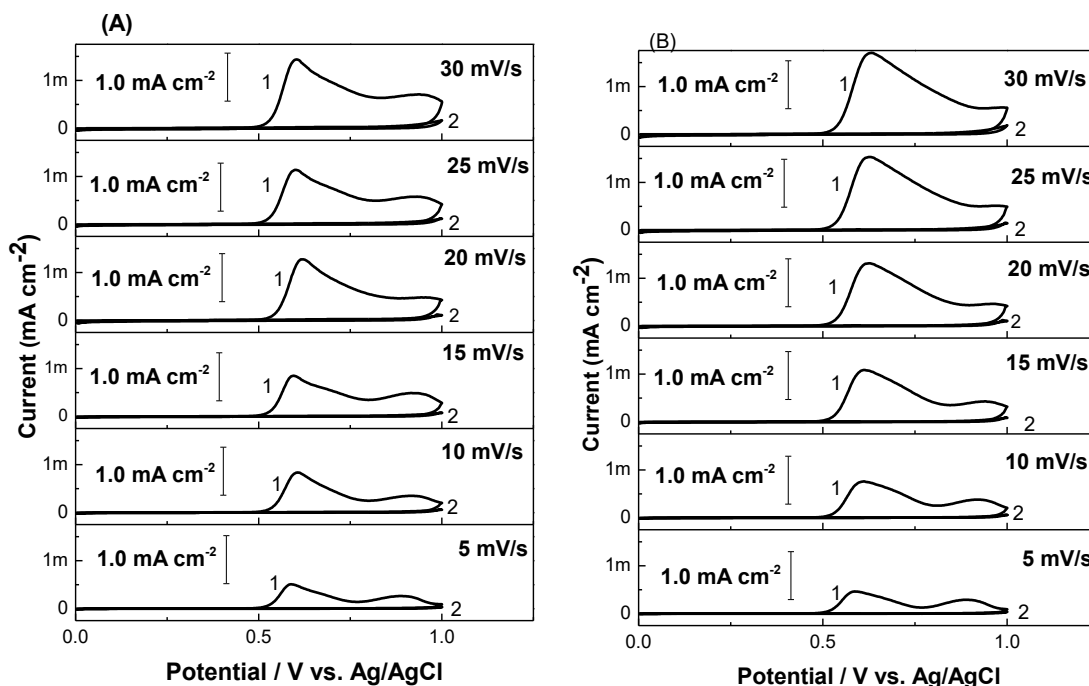


Figure 2. Electropolymerisation in 0.1 mol dm^{-3} sulfuric acid at $\text{pH}=1.2$ of 10 mmol dm^{-3} 2-nitrophenylenediamine (2NPPD) vs Ag/AgCl (3 mol dm^{-3} KCl). Cyclic voltammograms were obtained at a scan rate of 5 up to 30 mV s^{-1} (25 cycles) using (A) a bare 1.6 mm gold electrode ($A=0.02 \text{ cm}^2$), and (B) a bare 3 mm glassy carbon electrode ($A=0.07 \text{ cm}^2$). This figure presents the first and second cycles for every scan rate.

Yu and Khoo have presented a series of cyclic voltammograms for the oxidative polymerisation of 4.5 mmol dm^{-3} 4-nitro-1,2-phenylenediamine (4N_oPD) in 0.5 mol dm^{-3} H_2SO_4 , at the gold electrode.[9] Their first CV cycle revealed the presence of one irreversible oxidation peak, with a peak potential at $+0.81 \text{ V}$ in the first forward scan. The oxidation peak obtained by Yu and Khoo clearly arose from the oxidation of the monomer. As the polymer film was formed, the oxidation peak decreased with continuous cycling, demonstrating restricted access of the monomer to the electrode surface.[9] The authors found that, after many cycles, a small amount of monomer was being oxidised, as the current of the oxidation peak had not diminished completely.[9] Consequently, inspection of Figure 1 and 2 in the first cycle of each scan rate reveals an anodic oxidation peak that was observed at a range between 0.55 to 0.65 V , for both 5 and 10 mmol dm^{-3} 2NPPD monomer concentrations. The oxidation range obtained in the current study was lower than that obtained by Yu and Khoo.[9] Moreover, after 25 cycles, oxidation peak current densities decreased completely, to zero, from cycle number two. This indicates that all of the 2NPPD monomer was easily oxidised at the electrode surfaces.

Figure 3 presents the electrochemical behaviour of the bare electrodes, using 20 mmol dm^{-3} $\text{K}_3\text{Fe}(\text{CN})_6/\text{K}_4\text{Fe}(\text{CN})_6$, which consisted of 0.1 mol dm^{-3} KCl, versus (Ag/AgCl, 3 mol dm^{-3} KCl) at 20 mV s^{-1} (4 cycles). For the bare gold electrode, the peaks of the oxidation were observed at $+270 \text{ mV}$ ($3.5 \times 10^{-3} \text{ mA cm}^{-2}$) and the reduction was observed at $+181 \text{ mV}$ ($3.3 \times 10^{-3} \text{ mA cm}^{-2}$). Conversely, for the glassy carbon electrode, the peaks of the oxidation were observed at $+280 \text{ mV}$ ($3.1 \times 10^{-3} \text{ mA cm}^{-2}$) and the reduction was observed at $+176 \text{ mV}$ ($3.1 \times 10^{-3} \text{ mA cm}^{-2}$).

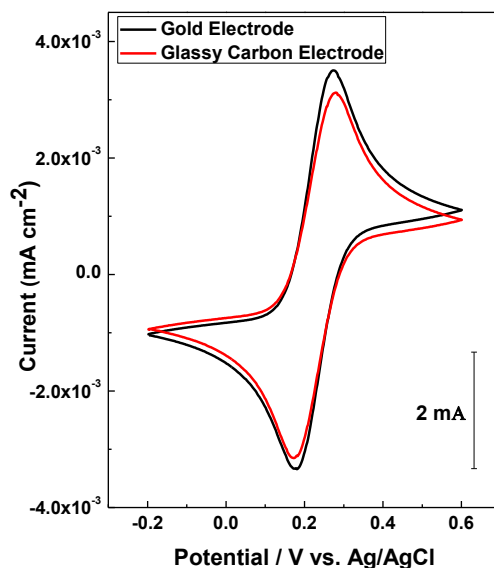


Figure 3. CV curves recorded for the bare electrodes using $20 \text{ mmol dm}^{-3} \text{ K}_3\text{Fe}(\text{CN})_6/\text{K}_4\text{Fe}(\text{CN})_6$ consisting of $0.1 \text{ mol dm}^{-3} \text{ KCl}$ vs Ag/AgCl ($3 \text{ mol dm}^{-3} \text{ KCl}$) at 20 mV s^{-1} (4 cycles). The black colour represents the CV curve for the bare gold electrode ($A=0.02 \text{ cm}^2$), and the red colour represents the bare glassy carbon electrode ($A=0.07 \text{ cm}^2$).

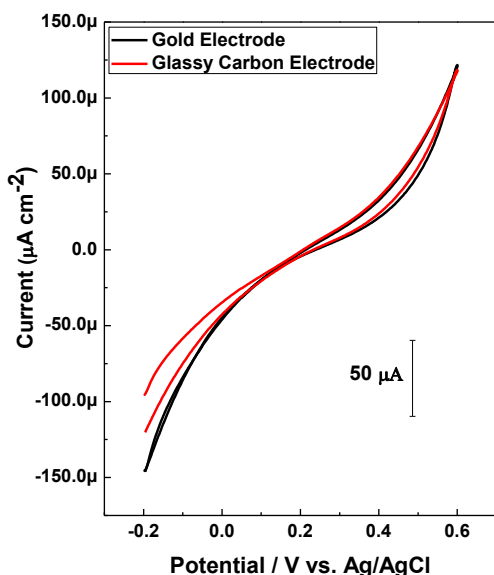


Figure 4. CV curves produced after testing the modified electrodes upon the electropolymerisation process in $20 \text{ mmol dm}^{-3} \text{ K}_3\text{Fe}(\text{CN})_6/\text{K}_4\text{Fe}(\text{CN})_6$ consisting of $0.1 \text{ mol dm}^{-3} \text{ KCl}$ vs Ag/AgCl ($3 \text{ mol dm}^{-3} \text{ KCl}$) at 20 mV s^{-1} (4 cycles). A 5 mV s^{-1} scan rate was used in the electropolymerisation with $5 \text{ mmol dm}^{-3} \text{ 2NPPD}$ in 0.1 mol dm^{-3} sulfuric acid at $\text{pH}=1.2$ vs Ag/AgCl ($3 \text{ mol dm}^{-3} \text{ KCl}$). The black colour represents the CV curve for the modified gold electrode ($A=0.02 \text{ cm}^2$), and the red colour represents the modified glassy carbon electrode ($A=0.07 \text{ cm}^2$).

After the electropolymerisation of 5 mmol dm^{-3} 2NPPD in 0.1 mol dm^{-3} sulfuric acid at $\text{pH}=1.2$, versus (Ag/AgCl, 3 mol dm^{-3} KCl) at 5 mV s^{-1} scan rate, the modified electrodes were tested in 20 mmol dm^{-3} $\text{K}_3\text{Fe}(\text{CN})_6/\text{K}_4\text{Fe}(\text{CN})_6$, which consisted of 0.1 mol dm^{-3} KCl, versus (Ag/AgCl, 3 mol dm^{-3} KCl) at 20 mV s^{-1} (4 sweeps). The CV results of the testing are presented in Figure 4. The CVs of the blocked electrode, as presented in Figure 4, were subsequently compared with the equal CVs of the bare electrodes, as presented in Figure 3. This comparison revealed that the current peaks that were related to the bare electrodes had diminished.

All the modified electrodes that were used to construct Figure 2 have been tested for passivation of the electrode's surfaces, by electropolymerisation in 20 mmol dm^{-3} $\text{K}_3\text{Fe}(\text{CN})_6/\text{K}_4\text{Fe}(\text{CN})_6$, which consisted of 0.1 mol dm^{-3} KCl, versus Ag/AgCl (3 mol dm^{-3} KCl) at 20 mV s^{-1} (4 sweeps). These CV results are presented in Figure 5. The concentration of the 2NPPD monomer was 10 mmol dm^{-3} and was electropolymerized in 0.1 mol dm^{-3} sulfuric acid at $\text{pH}=1.2$, versus Ag/AgCl, (3 mol dm^{-3} KCl).

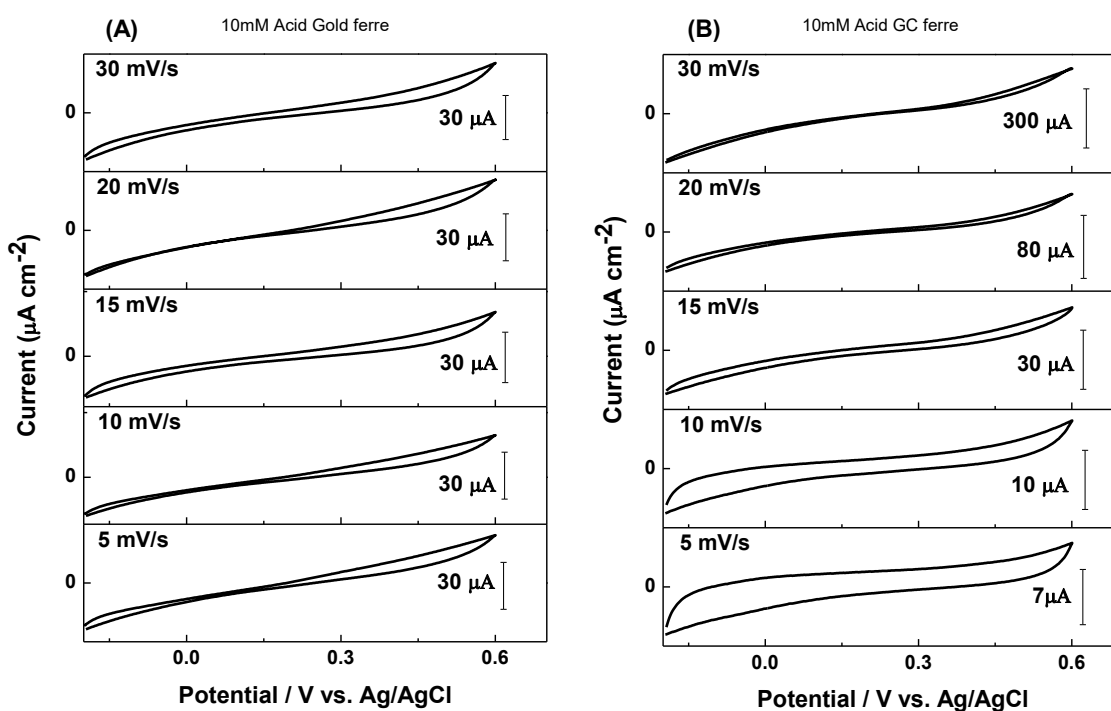


Figure 5. CV curves produced after testing the modified electrodes upon the electropolymerisation process in 20 mmol dm^{-3} $\text{K}_3\text{Fe}(\text{CN})_6/\text{K}_4\text{Fe}(\text{CN})_6$ consisting of 0.1 mol dm^{-3} KCl vs Ag/AgCl (3 mol dm^{-3} KCl) at 20 mV s^{-1} (4 cycles). Each scan rate is linked to the scan rate used in the electropolymerisation process with 10 mmol dm^{-3} 2NPPD in 0.1 mol dm^{-3} sulfuric acid at $\text{pH}=1.2$ vs Ag/AgCl (3 mol dm^{-3} KCl). (A) 1.6 mm gold modified electrode ($A=0.02 \text{ cm}^2$) and (B) 3 mm modified glassy carbon electrode ($A=0.07 \text{ cm}^2$).

In Figure 5, CVs demonstrated a similar behaviour to that of the distinct predisposition absence of angle peaks, for both types of electrodes that were used. All CVs experienced a drop in anodic current peaks in the micro ampere of 30 µA/cm^2 for gold electrodes, as depicted in Figure 5. For the glassy carbon electrodes, a CV experienced a drop in the anodic current peak in the micro ampere of 7 µA/cm^2 at 5 mV/s , and increased gradually up to 300 µA/cm^2 at 30 mV/s . This occurrence is related to the

electropolymerisation of the 2NPPD monomer, as an insulating polymer layer was electrochemically formed at the surface of both of the materials of the electrodes used.

Table 4 illustrates the diffusion coefficients for the 2NPPD monomer, which were calculated from the first cycle of the electropolymerisation CVs, at different scan rates that ranged from 5 to 30 mV s⁻¹. This revealed that, with an increasing scan rate, the peak current (i_p) increased linearly, with the square root of the potential scan rate ($v^{1/2}$). This confirms that the electropolymerisation of the 2NPPD monomer is a linear diffusion-controlled process. The diffusion coefficients were measured using the Randles-Sevcik equation (Eq. 1): [19, 20]

$$I_p = (2.69 \times 10^5)n^{3/2}A\sqrt{D}\sqrt{v}C \dots \text{Eq. 1}$$

where I_p is the peak current maximum in amps, n is the number of electrons in the event, A is the surface area of the working electrode in cm², D is the diffusion coefficient of the electroactive species in cm²/s, v is the scan rate of voltammograms in V/s, and C is the bulk concentration of the electroactive species mol/cm³.

Table 4. Calculated values of diffusion coefficients.

Monomer concentration	Diffusion Coefficients cm ² s ⁻¹ × 10 ⁻⁵	
	Gold electrode	Glassy carbon electrode
5 mmol dm ⁻³ 2NPPD	1.7	1.5
10 mmol dm ⁻³ 2NPPD	0.8	1.1

Examination of Table 4 also indicated that, when the monomer concentration of 2NPPD was increased, the calculated diffusion coefficients for gold and glassy carbon electrodes decreased. This could relate to the lower solubility of the 2NPPD monomer in acidic solutions and, preferably, electropolymerisation of the monomer at low concentrations.

Figure 6 illustrates the relationship between the first anodic current density and the square root of the scan rates of the modified gold electrodes, for 5 and 10 mmol dm⁻³ of the 2NPPD monomer concentrations. The first anodic peaks in the first cycle of the CVs are presented in Figures 1A and 2A, are used to build up the plots. A linear relationship was obtained and the correlation coefficient values were R²=0.9968 for 5 mmol dm⁻³ and R²=0.9912 for 10 mmol dm⁻³ 2NPPD, with a zero intercept.

Figure 7 depicts the relationship between the first anodic current density and the square root of the scan rates of the modified glassy carbon electrodes, for 5 and 10 mmol dm⁻³ of the 2NPPD. The first anodic peaks are presented in Figures 1B and 2B, are used to construct the plots. A linear relationship was obtained and the correlation coefficient values were R²=0.9991 for 5 mmol dm⁻³ and R²=0.9945 for 10 mmol dm⁻³ 2NPPD, with a zero intercept.

The intercept in Figures 6 and 7 was equal to zero. This value could be attributed to a decrease in the active area of the working electrode during electropolymerisation, as the positive CV scan

proceeds. This means the polymer layers increased, which blocked the active area of the working electrode.

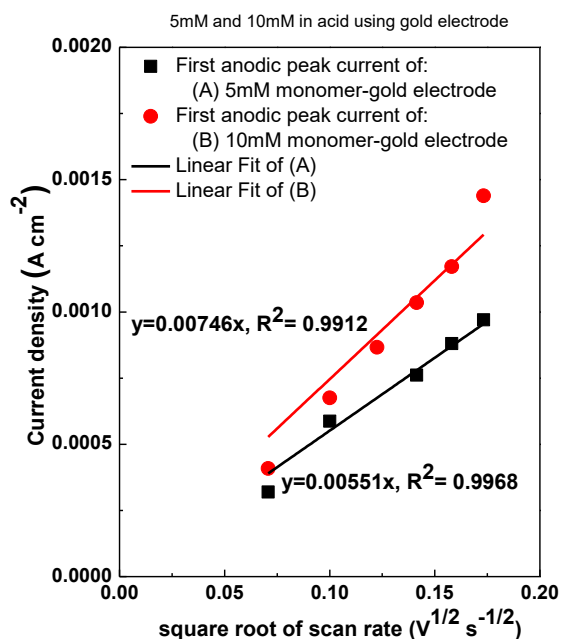


Figure 6. The plot of anodic current density vs the square root of the scan rates of the modified gold electrodes ($A=0.02\ cm^2$) under $0.1\ mol\ dm^{-3}$ sulfuric acid at $pH=1.2$. The black line represents the first anodic peak current of $5\ mmol\ dm^{-3}$ 2NPPD and its corresponding linear fit ($R^2=0.9968$). The red line represents the first anodic peak current of $10\ mmol\ dm^{-3}$ 2NPPD and its corresponding linear fit ($R^2=0.9912$).

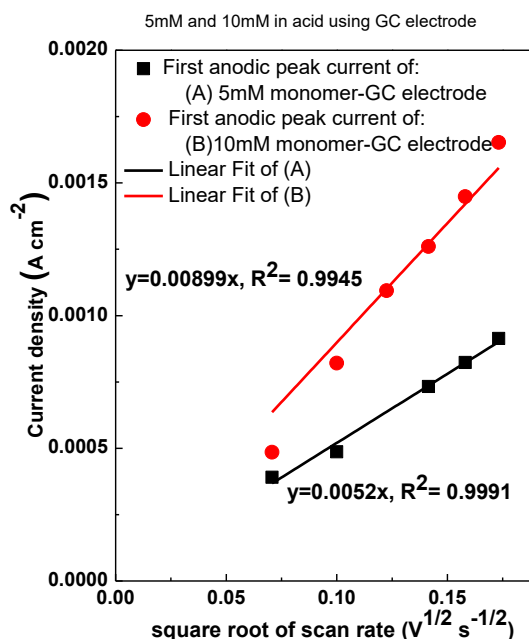


Figure 7. The plot of the first anodic current density vs the square root of the scan rates of the modified glassy carbon electrodes ($A=0.07\ cm^2$) under $0.1\ mol\ dm^{-3}$ sulfuric acid at $pH=1.2$. The black line shows the first anodic peak current of $5\ mmol\ dm^{-3}$ 2NPPD and its corresponding linear fit ($R^2=0.9991$). The red line shows the first anodic peak current of $10\ mmol\ dm^{-3}$ 2NPPD and its corresponding linear fit ($R^2=0.9945$).

SEM images of the bare gold-coated Si-chips electrode and blocked gold-coated Si-chips electrode with poly 2NPPD are presented in Figures 8a and 8b, respectively. Both images were captured at the same magnification of 1.0 KX magnifications. Although the bare gold surfaces are largely featureless, the surface morphology of the poly 2NPPD surfaces showed faint scratches, which appear similar to a tree-like structure. The morphological features of the poly 2NPPD surface revealed large, melted, disordered patterns. These surfaces contained large areas of distinguishable faint and dark irregular regions. As the poly 2NPPD films are very thin, they appear different when compared to the bare gold surfaces.

The capability of the design expert enables the model, by providing interaction plots between the two studied factors (Figure 9) and the normal probability plots versus the studentised residuals (Figure 10).

Figure 9 presents the interaction plot of the electrode type versus the scan rate (mV s^{-1}) in the electropolymerisation of 10 mmol dm^{-3} 2NPPD under 0.1 mol dm^{-3} sulfuric acid at $\text{pH}=1.2$. The first anodic current density in μAcm^{-2} was plotted in the y-axis, which represented the response. Figure 9 indicates that the current densities increased proportionally as the scan rate increased. The greatest value was obtained at the upper level of all factors. Parallel lines at the interactions' plot indicate a lack of interaction among those factors, whereas secant lines confirm interaction [21]. Hence, no secant lines were observed in this figure, which led to a lack of interactions between both of the electrodes' materials that were used, as the interaction lines were parallel to each other.





Figure 8. SEM images of gold-coated Si-chips ($A=1.0\text{ cm}^2$) at 1.0 KX magnification of: (A) bare gold electrode and (B) blocked gold electrode upon the electropolymerisation of 10 mmol dm^{-3} 2-nitro-p-phenylenediamine (0.1 mol dm^{-3} KCl) using CV vs Ag/AgCl at 5 mV s^{-1} scan rate (25 cycles) in acidic solution ($\text{pH}=1.2$).

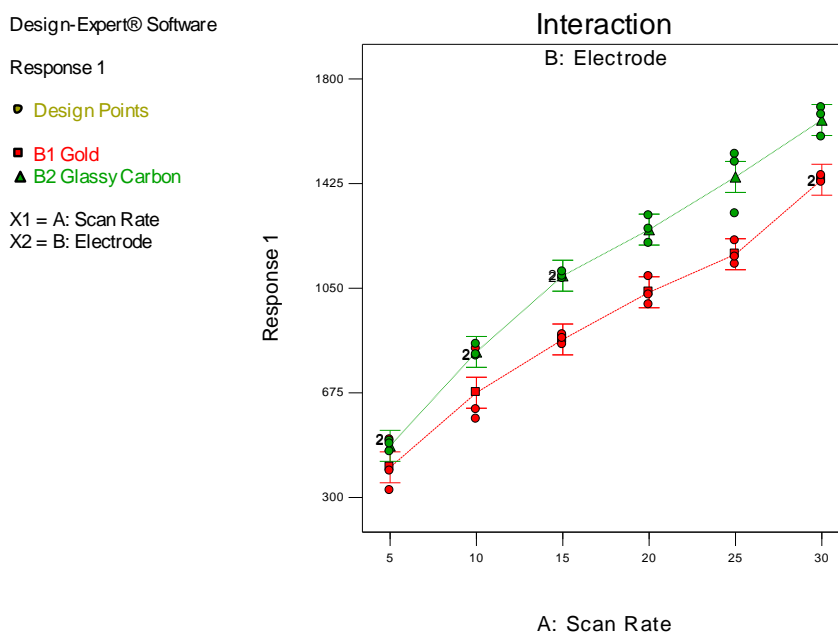


Figure 9. Interaction plot of the electrode type vs the scan rate (mV s^{-1}) in the electropolymerisation of 10 mmol dm^{-3} 2NPPD under 0.1 mol dm^{-3} sulfuric acid at $\text{pH}=1.2$. Response 1 is the first anodic current density in μAcm^{-2} . Electrode types used are gold electrodes ($A=0.02\text{ cm}^2$) marked in red and glassy carbon electrodes ($A=0.07\text{ cm}^2$) marked in green.

Observation of Figure 10 suggests that the normal probability plot of residuals resulted in a straight line, since the underlying error distribution is normal. Therefore, the normality assumption was valid for our proposed model. As noted in Figure 10, data was distributed normally, as the residuals were

intensified in the middle of the straight line and showed no significant deviation from the residuals. This could be accepted as an indicator of outliers that are contained in this region.

A previous study conducted by Cataldo reports that p-phenylenediamine (PPD) does not polymerise in non-aqueous solvents.[22] Having investigated the electrochemical behaviour of PPD by CV in aqueous acidic medium,[23] the author conducted the experiments using $0.1 \text{ mol dm}^{-3} \text{ HClO}_4$ and $0.05 \text{ mol dm}^{-3} \text{ PPD}$, and by using two platinum electrodes and an Ag/AgCl as a reference electrode. Cataldo reported an initial oxidation of the PPD monomer, which he observed by the formation of a bluish cation radical on the electrode surface.[23] He indicated that the occurrence of continuous oligomerisation upon consecutive cycles, in both cathodic and anodic currents, increased consistently. However, after ten cycles, he noticed that no further current growth was observed. Cataldo subsequently asserts that only a very low molar mass product was deposited in these conditions. Therefore, it could not adhere to the electrode's surface, and was instead dispersed in the surroundings.[23] However, Cataldo has shown that PPD could be polymerised chemically, by the action of an oxidising agent, such as $\text{K}_2\text{S}_2\text{O}_8$. By means of electronic spectroscopy, the author followed the oxidation of PPD in HCl acid solution with $\text{K}_2\text{S}_2\text{O}_8$ added at 1: 1 molar ratio.[23]

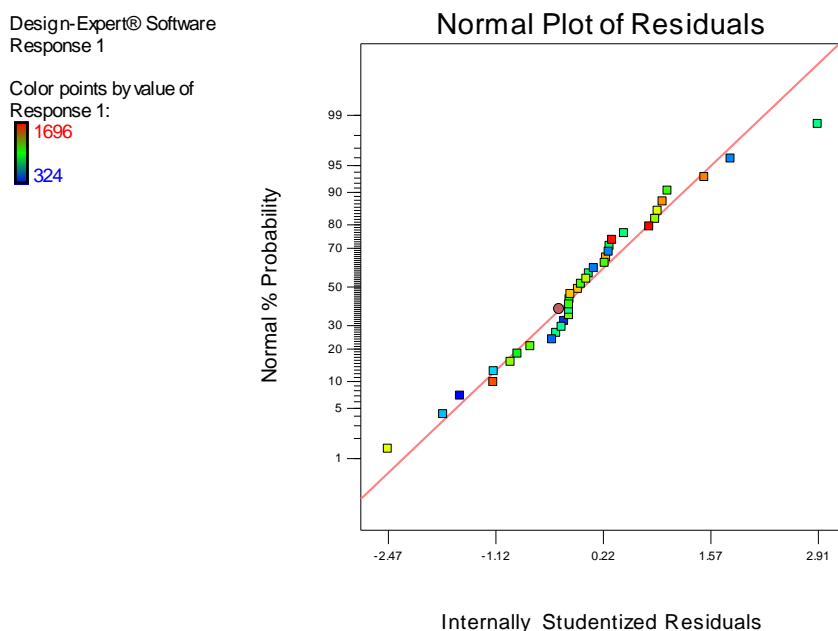
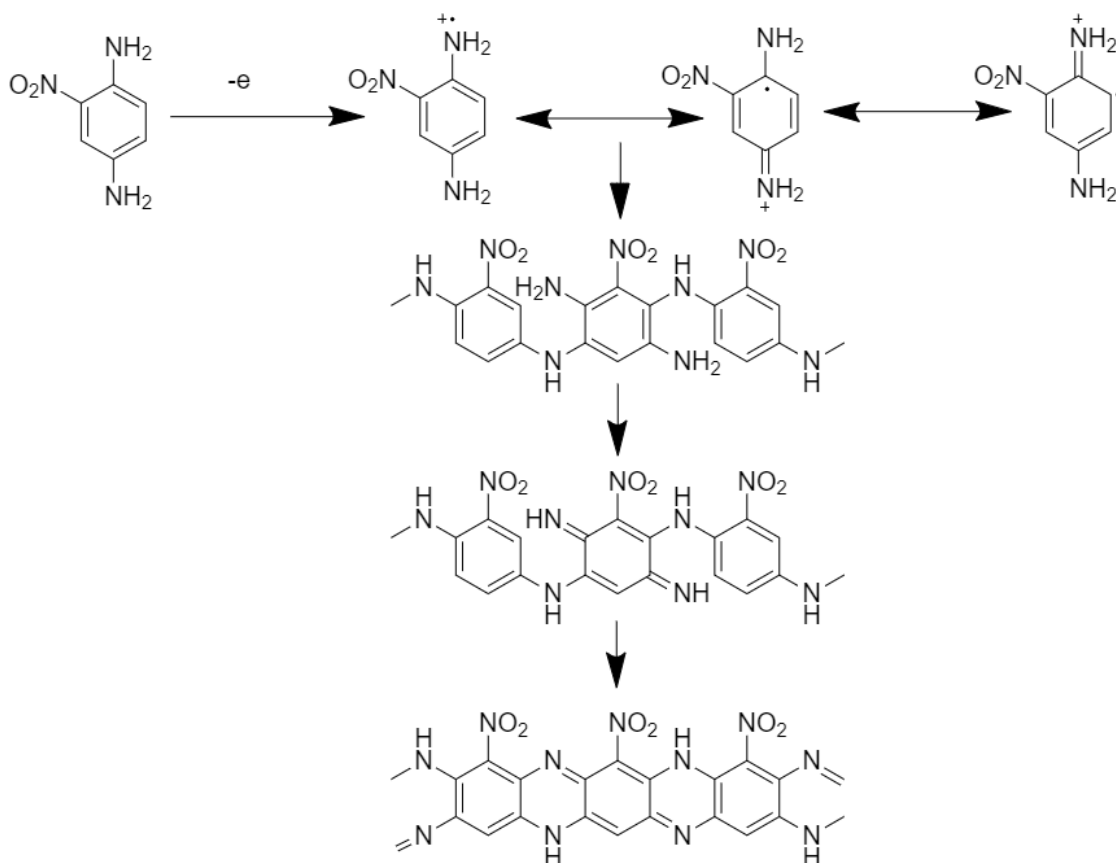


Figure 10. Normal probability vs studentised residuals for checking normality of residuals.

The current study returned results that were different from Cataldo's study, as previously discussed. The 2NPPD monomer revealed different CV scans, as the distinguished anodic current peak observed in the first cycle was diminished in the second cycle. This phenomena was extensively observed during our work in the laboratory. We assert that this phenomena was due to a thin film deposition on the electrode's surface and consequent electropolymerisation.[24-28] As previously indicated in Figure 5, all the modified electrodes were immersed and tested in the presence of a $\text{K}_3\text{Fe}(\text{CN})_6 / \text{K}_4\text{Fe}(\text{CN})_6$ redox couple. All the CV traces recorded were different from the original CV,

when compared to Figure 3, and experienced a drop in anodic current range, without a distinct inclination of angle peaks. The electrochemical change can be explained by a passivation of the electrode surface, which prevents reduction of ferricyanide, as opposed to electrostatic repulsion. This phenomenon was related to the electropolymerisation of the 2NPPD monomer, as a thin layer of an insulating polymer was electrochemically deposited on the surfaces of the gold and glassy carbon electrodes.



Scheme 1. Oxidation of 2NPPD monomer

In general, the oxidation of the 2NPPD monomer in acidic solutions first proceeds by an extraction of an electron from the lone pair on the nitrogen atom of the amine group, with the formation of radical cation, as shown in Scheme 1. The stability of the initially formed radical cation could be affected, due to the NO_2 group substituent at the benzene ring. This could be attributed to the strong electron withdrawing nature of the NO_2 group, which could somehow affect the following coupling reactions. However, the radical cation formed upon the oxidation of the 2NPPD monomer was stabilised by resonance (as shown in Scheme 1) but with a deep colour that tended to undergo electropolymerisation. In the radical cation, the active sites were available at the ortho positions of the two amino groups present in each molecule, whereas the para positions were blocked (Scheme 1). Hence, we propose the initial formation of a polyaniline with a substituted nitro leucoemeraldine, which then further developed into a substituted nitro pernigraniline-type polymer.

Table 5 presents the analysis of variance (ANOVA) of the partial sum of squares for the selected factorial model. ANOVA could be useful for the adequacy of the model. Using an F-test enables the estimation of the main and interaction effect degrees between factors. Table 5 lists the F-test and significance values, employed to test the overall model, the scan rate individual component (A), the electrode material type's individual component (B), and the interactions between AB.

Table 5. ANOVA table (partial sum of squares) for selected factorial model [Classical sum of squares - Type II]

ANOVA for selected factorial model						
Source	Sum of Squares	DF	Mean Square	F Value	p-value Prob > F	
Model	5.1×10 ⁶	11	4.6×10 ⁵	106.2	< 0.0001	significant
A-Scan Rate	4.7×10 ⁶	5	9.4×10 ⁵	216.1	< 0.0001	
B-Electrode	3.4×10 ⁵	1	3.4×10 ⁵	78.6	< 0.0001	
AB	38051.2	5	7610.2	1.8	0.16	
Pure Error	1.0×10 ⁵	24	4334.5			
Cor Total	5.2×10 ⁶	35				

The 106.2 F-value meant that the model was significant. Due to noise, there was only a 0.01% chance that a *Model F-Value* could occur. Values of *Prob > F* found to be less than 0.05 indicate that the model terms were significant. In this case, A and B factors are significant model terms. Values greater than 0.10 indicate that the model terms are not significant. The following is the final equation in terms of coded factors:

$$\text{Response } (\mu\text{Acm}^{-2}) = + 1029.8 - 583.3 * A[1] - 281.3 * A[2] - 49.3 * A[3] + 117.8 * A[4] + 80.3 * A[5] + 97.3 * B - 58.8 * A[1]B - 24.1 * A[2]B + 16.9 * A[3]B + 15.1 * A[4]B + 41.2 * A[5]B$$

It was noted that the predicted R² of 0.9547 was in reasonable agreement with the adjusted R² of 0.9706. In other words, adequate precision measures the signal to noise ratio. A ratio greater than 4 is desirable. The current model ratio of 26.9 indicates that an adequate signal was obtained. Future studies could use our model to navigate the design space.

4. CONCLUSION

This paper reports the feasibility of the electrodeposition of the thin polymeric films of 2NPPD, at the surfaces of gold and glassy carbon electrodes, in acidic aqueous solutions of pH=1.2. The poly 2NPPD films were very thin, and thus different, when compared to the bare gold surfaces.

A general factorial design was conducted, in order to provide insight into the parameters of electropolymerisation. The interaction plots between the studied factors of the scan rates and the

electrode's type of materials revealed that the current densities increased proportionally as the scan rate increased. However, there was no interaction between both of the studied electrodes' materials.

In all CV scans of the 2NPPD monomer, a rapid drop in the anodic current peak was proposed as an indication of electropolymerisation. Further examination of the modified electrode's surfaces was conducted by running a CV scan in $K_3Fe(CN)_6/K_4Fe(CN)_6$ solution. The CV results demonstrated that the electrode's surfaces were successfully coated and blocked by the polymer, as the current peaks that related to the bare electrodes had diminished.

Morphological features, which were similar to tree-like structures with faint scratches, were observed on the electrode's surfaces. The calculated diffusion coefficients confirmed that the electropolymerisation of the 2NPPD monomer followed a linear diffusion-controlled process. It was subsequently noted that, when the monomer concentration decreased, the calculated diffusion coefficients decreased.

ACKNOWLEDGEMENTS

The authors are grateful to the College of Engineering at the University of Business and Technology (UBT), Jeddah, Saudi Arabia.

References

1. E.G. Cansu Ergun, D. Eroglu, *Org. Electron.*, 75 (2019) 105398.
2. H.E. Elkhidr, Z. Ertekin, Y.A. Udum, K. Pekmez, *Synth. Met.*, 260 (2020) 116253.
3. V. Figà, H. Usta, R. Macaluso, U. Salzner, M. Ozdemir, B. Kulyk, O. Krupka, M. Bruno, *Opt. Mater.*, 94 (2019) 187-195.
4. S.-H. Hsiao, Y.-Z. Chen, *Eur. Polym. J.*, 99 (2018) 422-436.
5. R. Kirankumar, W.-C. Huang, H.-F. Chen, P.-Y. Chen, *J. Electroanal. Chem.*, 826 (2018) 198-206.
6. A. Kushwaha, N. Gupta, J. Srivastava, A.K. Singh, M. Singh, *Microchem. J.*, 152 (2020) 104355.
7. D. Vanossi, L. Pigani, R. Seeber, P. Ferrarini, P. Baraldi, C. Fontanesi, *J. Electroanal. Chem.*, 710 (2013) 22-28.
8. S.M. Sayyah, S.S. Abd El-Rehim, S.M. Kamal, M.M. El-Deeb, R.E. Azooz, *J. Appl. Polym. Sci.*, 119 (2011) 252-264.
9. B. Yu, S.B. Khoo, *Electrochim. Acta*, 50 (2005) 1917-1924.
10. M.A. Kamyabi, N. Rahmanian, *Anal. Methods*, 7 (2015) 1339-1348.
11. C.d.C. Santos, T.C. Pimenta, R.L. Thomasini, R.M. Verly, D.L. Franco, L.F. Ferreira, *J. Electroanal. Chem.*, 846 (2019) 113163.
12. C. Hu, Y. Li, T. Li, Y. Qing, J. Tang, H. Yin, L. Hu, L. Zhang, Y. Xie, K. Ren, *Colloids Surf., A*, 585 (2020) 124176.
13. S. Lakard, J. Husson, S. Monney, C.C. Buron, B. Lakard, *Prog. Org. Coat.*, 99 (2016) 429-436.
14. H. Hrichi, L. Monser, N. Adhoum, *J. Electroanal. Chem.*, 805 (2017) 133-145.
15. S.M. Sayyah, M.M. El-Deeb, *J. Appl. Polym. Sci.*, 103 (2007) 4047-4058.
16. H.M. Mousa, J.R. Aggas, A. Guiseppi-Elie, *Mater. Lett.*, 238 (2019) 267-270.
17. J.J. Yourick, R.L. Bronaugh, *Toxicol. Appl. Pharmacol.*, 166 (2000) 13-23.
18. A.S. Barham, *Int. J. Electrochem. Sci.*, 13 (2018) 3660-3673.
19. J.E.B. Randles, *Trans. Faraday Soc.*, 44 (1948) 327-338.
20. A. Sevick, *Collect. Czech. Chem. Commun.*, 13 (1948) 349-377.
21. P. García-Manrique, M.B. González-García, M.C. Blanco-López, Chapter 35 - Design of

experiments at electroanalysis. Application to the optimization of nanostructured electrodes for sensor development, in: M.T. Fernandez Abedul (Ed.) *Laboratory Methods in Dynamic Electroanalysis*, Elsevier, 2020, pp. 361-371.

22. P. Chandrasekhar, R.W. Gumbs, *J. Electrochem. Soc.*, 138 (1991) 1337-1346.
23. F. Cataldo, *Eur. Polym. J.*, 32 (1996) 43-50.
24. A.S. Barham, *J. Electrochem. Soc.*, 162 (2015) G36-G40.
25. A.S. Barham, *J. New Mat. Electrochem. Syst.*, 18 (2015) 037-041.
26. A.S. Barham, *Int. J. Electrochem. Sci.*, 10 (2015) 4742-4751.
27. A.S. Barham, B.M. Kennedy, V.J. Cunnane, M.A. Daous, *Int. J. Electrochem. Sci.*, 9 (2014) 5389-5399
28. A.S. Barham, B.M. Kennedy, V.J. Cunnane, M.A. Daous, *Electrochim. Acta*, 147 (2014) 19-24

© 2020 The Authors. Published by ESG (www.electrochemsci.org). This article is an open access article distributed under the terms and conditions of the Creative Commons Attribution license (<http://creativecommons.org/licenses/by/4.0/>).